Indian Academy of Sciences Conference Series (2020) 3:1
DOI: 10.29195/iascs.03.01.0024

Signatures of climatic phenomena in climate networks: Cyclones, El Niño and La Niña

RUPALI SONONE, RUBY SAHA and NEELIMA GUPTE*

Department of Physics, Indian Institute of Technology Madras, Chennai 600 036, India
*Corresponding author. E-mail: gupte@physics.iitm.ac.in

Abstract. We construct climate networks based on surface air temperature data to identify distinct signatures of climatic phenomena such as cyclones, El Niño and La Niña events which trigger many climatic disruptions around the globe with serious economic and ecological consequences. The climate network shows a discontinuous phase transition in the size of the normalised largest cluster and the susceptibility during cyclones. The correlation matrix of the network shows a structure which has distinct characteristics of El Niño events, La Niña events, and no events. We also identify the signature of the El Niño and La Niña oscillations in the heat map of the system. We discuss further analysis of these systems.

Keywords. Climate networks; El Ninõ; La Ninã; cyclones.

PACS Nos 92.60.hv; 05.40.-a; 89.75.-k

1. Introduction

The construction and study of complex networks based on climate data is a novel and efficient approach to study climate systems [1–3]. This has led to the development of percolation based measures to study and quantify climate networks [1]. Climatic phenomena have major consequences for ecological and economic events. Hence the prediction of climatic phenomena is of enormous practical utility but is quite difficult due to the complex and nonlinear nature of the phenomena under consideration. These climate networks are constructed using massive datasets consisting of the time series of weather observations at different geographic locations. Tracking structural changes in the climate network of temperatures shows signature features of upcoming climatic events such as El Niño events and cyclones. Tracking and quantifying the structural changes and signature features in these climate networks can be used to identify precursors of the upcoming climatic event.

The climate system can be represented by a grid of oscillators, with each oscillator reflecting a complex time series of certain weather observations such a wind velocity, precipitation, surface temperature, etc. Climate networks are used to forecast various important climate phenomena, such as the monsoon, the North Atlantic oscillation, El Niño events and cyclones [4, 5].

Here we use correlation networks constructed out of the surface air temperature of time series of different points in a global grid to analyse climatic phenomena of two distinct classes: cyclones in the Indian Ocean and the El Niño and La Niña phenomena. We demonstrate the signatures of these phenomena in different quantities. In the case of the cyclone, we identify the signatures of the cyclone in the order parameter and the susceptibility of the corresponding correlation network. In the case of the La Niña and El Niño oscillations, we identify the signature of the oscillations in the heat map of the system. We first discuss the analysis of cyclonic events.

2. Cyclones

A tropical cyclone (TC) is a large-scale air mass with inward spiralling winds rotating around a strong center of low atmospheric pressure that originates over the warm tropical ocean. It lasts up to 3–7 days. We observe a bi-modal TC season in the Indian Ocean basin. The two modes are

1. Pre-monsoon: March–April–May
2. Post-monsoon: October–November–December (maximum TC frequency; stronger wind velocities)

Currently cyclones can be predicted up to seven days in advance.

We construct a climate network which is based on near surface air temperature data collected at 1000 hPa, nearly equal to one atmospheric pressure, at the grid points (nodes) of a geographic grid based on latitude and

longitude values (ERA-interim reanalysis data, downloaded from [6]) for the years 2013–2018. We have considered a network grid located between 30°E and 110.25°E longitudes, and 35.25°N and 35.25°S latitudes with a grid size resolution of 0.75°S (≈83 km). This grid resolution gives us a total number of 10,260 nodes scattered uniformly in the Indian Ocean.

The climate network is constructed based on the similarity of the dynamics between the nodes as measured by the correlation coefficient [1, 7].

Using the given grid size and parameters mentioned above, we constructed networks for the months of October, November and December 2016 (two networks for each month, a total of six networks) using the correlation coefficient defined below. The normalised cluster size and susceptibility are then obtained. We obtain consistent and promising results for the year 2016 showing some signatures of the upcoming cyclones in the plots of the normalized largest cluster and the susceptibility as functions of the correlation coefficient.

The details of construction are as follows: We calculate the quantity $T_i(d)$ from the measured near surface temperature $\tilde{T}_i(d)$ at the grid location i, on the day d, and the cross-correlation function $C_{i,j}$ using the relations

$$T_i(d) = \frac{\tilde{T}_i(d) - \text{mean}(\tilde{T}_i(d))}{\text{std}(\tilde{T}_i(d))} \tag{1}$$

$$C_{i,j}(\tau) = \frac{\langle T_i(d-\tau)T_j(d)\rangle - \langle T_i(d-\tau)\rangle\langle T_j(d)\rangle}{\sqrt{(T_i(d-\tau) - \langle T_i(d-\tau)\rangle)^2}.\sqrt{(T_j(d) - \langle T_j(d)\rangle)^2}}, \tag{2}$$

where 'mean' and 'std' are the mean and standard deviation of the temperature on day d over all years (2013–2018) and τ is the time lag taken here to be between 0 and 7 days, with eq. (1) being implemented for the temperature at each site i. Only the temperature data points prior to day 'd' are considered. The averages ($\langle\ \rangle$) are taken over 15 days. Here the labels i and j denote two distinct nodes in the geographical grid. The weight of the link between i and j is defined as the maximum of the cross-correlation function, $\max(C_{i,j}(\tau))$. Here, links were added one by one with decreasing link strength, i.e. the links or edges with the highest weight (the maximum value of the cross-correlation function, $C_{i,j}$) are added first to the network. Further edges are added in order by decreasing weight. Thus the network evolves as a function of C, as links of weights ranging from a given value of C up to the maximum value of C are added at each stage. Quantities such as the order parameter, which is the normalized size of the largest cluster (s_1) and the susceptibility (χ) for each distinct value of C are studied. These are defined by the relations

$$s_1 = \frac{S_1}{N} \tag{3}$$

$$\chi = \frac{\sum_s' s^2 n_s(C)}{\sum_s' s n_s(C)}. \tag{4}$$

Here, S_1 is the size of largest cluster, or collection of linked nodes, N is the total number of nodes in the network, $n_s(C)$ is the number of clusters of size s for a given value of C, and the prime on the sums indicates the exclusion of the largest cluster S_1 in each measurement. The susceptibility of the network gives the measure of the spread in the sizes of clusters which appear at a given correlation strength.

The plots show some distinctive discontinuities in the order parameter s_1 during cyclones. The order parameter s_1 shows discontinuous jumps in the pre-cyclone period 1st to 15th October and the cyclone period 16th to 31st October, 2016 (cyclone Kyant figure 1). After the cyclone, in the period 1st to 15th November, the discontinuities smooth out (figure 2a). From 16th to 30th November, the signatures of cyclone Nada start showing in the order parameter (29th November to 2nd December, figure 2b). Figures 3a and b, which correspond to the period 1st to 15th December and 16th to 30th December, 2016 contain the signatures of the build-up to the severe cyclone Vardah, and the cyclone itself (6th to 18th December).

The susceptibility plots show up these features even more strongly. We observe multiple peaks in the susceptibility χ (blue) for the networks (such as 1st to 15th October and 1st to 15th November) before cyclones (figures 1a and 2a). The values of the susceptibility peaks are quite small (15 and 30) for these networks. We observe distinct sharp peaks and much higher values of susceptibility (80 and 330) for the networks (such as 16th to 31st October and 16th to 30th November (figures 1b and 2b)) during the period of the cyclone. We also observe sharp distinct peaks and higher susceptibility values for both the networks in the month of December as there is an overlap of two cyclonic storms Nada (29 Nov–2 Dec) and Vardah (6–18 Dec) for the network constructed for 1st to 15th December (figures 3a and b).

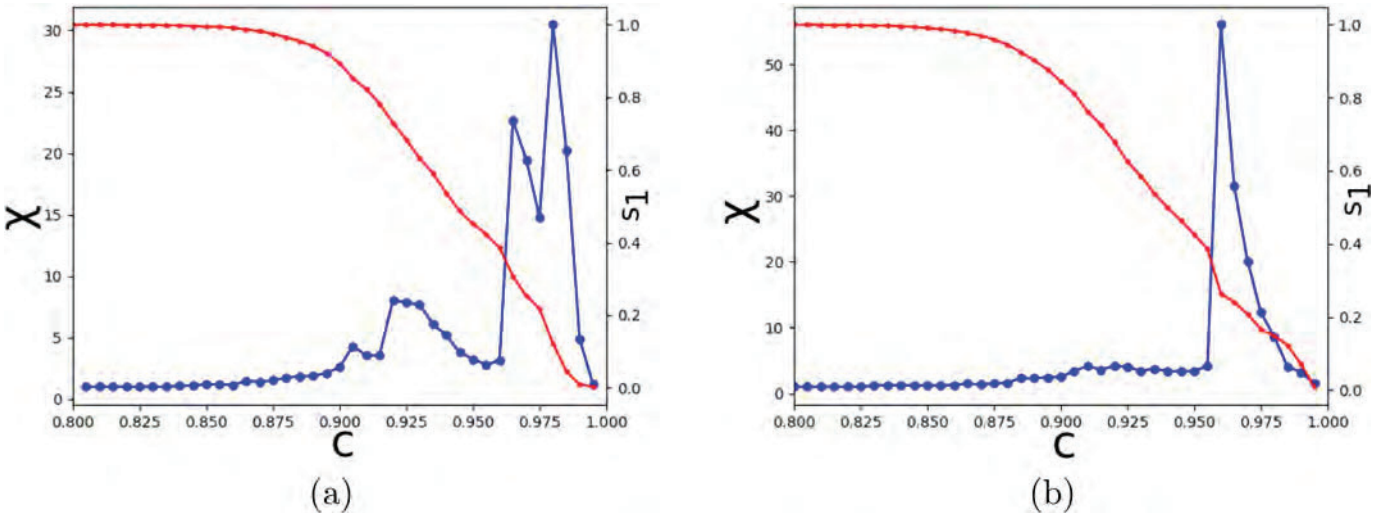

Figure 1. The normalised largest cluster s_1 (red) and susceptibility χ (blue) as a function of the link strength C for the network (**a**) 1st to 15th October, 2016 and (**b**)16th to 31st October, 2016. Cyclone Kyant (21–27 October).

We intend to verify results for other years and construct networks based on other relevant parameters such as networks of daily datasets of air temperature at 850 hPa, sea level pressure, meridional wind at lower level ($V850$) and zonal wind at upper and lower tropospheric levels ($U200$, $U850$), etc.

We note that the percolation based method has been used to analyse El Niño and La Niña phenomena and has been used to obtain successful predictors of the El Niño [8–10]. Similar methods have been used for bifurcations in models of lake eutrophication, the Ginzburg Landau system and others. It remains to be seen if successful predictors can be constructed for cyclones.

3. El Niño and La Niña events

We also demonstrate the analysis of climate networks for the El Niño and La Niña phenomena by a different method. We analyse the correlation matrix constructed from the time series and use the strength of the correlations to construct a heat map. The signature of the El Niño and La Niña events is seen in the heat maps, as we will see here.

The El Niño oscillation is a major climatic event which occurs across the central and east-central equatorial Pacific. An El Niño event is the warmer phase, and a La Niña event is the colder phase of the El Niño southern oscillation. On the appearance of El Niño the

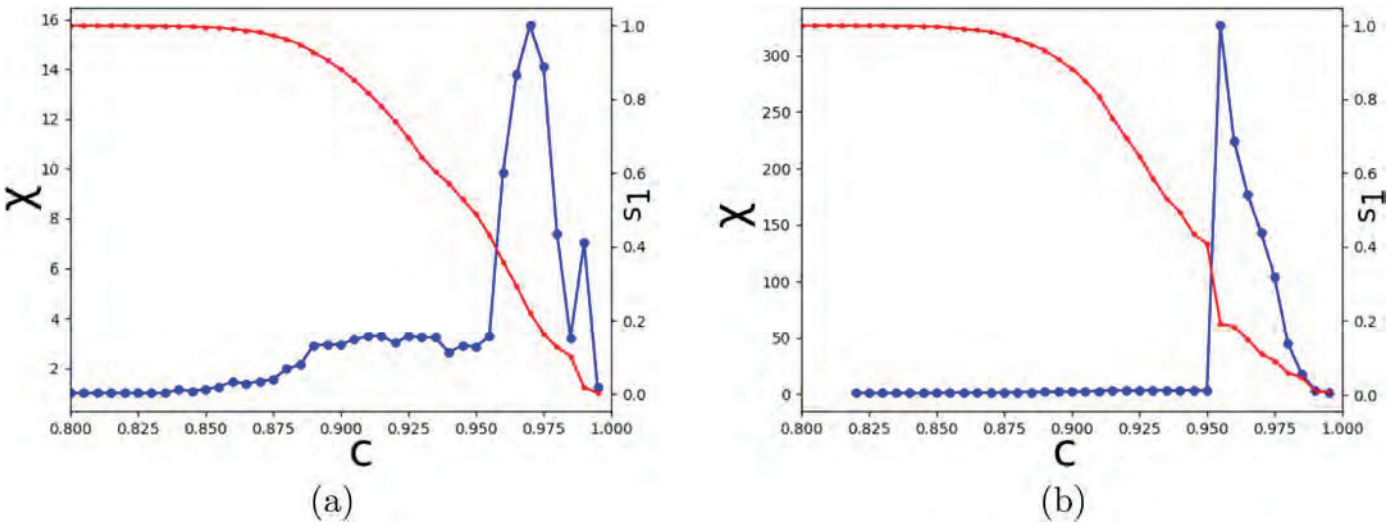

Figure 2. The normalised largest cluster s_1 (red) and susceptibility χ (blue) as a function of the link strength C for the network (**a**) 1st to 15th November, 2016, (**b**)16th to 30th November, 2016. Cyclone Nada (29 November to 2 December).

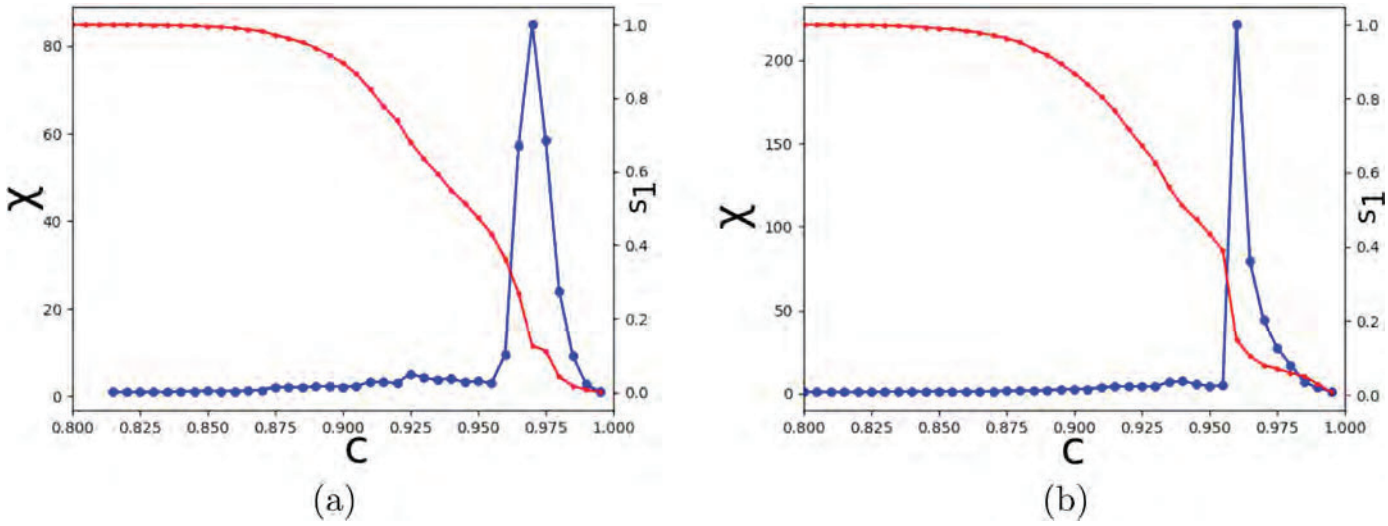

Figure 3. The normalised largest cluster s_1 (red) and susceptibility χ (blue) as a function of the link strength C for the network (**a**)1st to 15th December, 2016. Cyclone Vardah (6–18 December) (**b**) 16th to 31st December, 2016.

eastern Pacific Ocean gets warmer by several degrees. The La Niña event is the cold anomaly over the same region. The Oceanic Niño index (ONI) is a measure of this anomaly [11].

Here, we use reanalysis data of the daily near surface air temperature (1000 hPa) from the 'NCEP/NCAR reanalysis 1 project' (1979–2019) (https://psl.noaa.gov/). We pick 725 grid points with (7.5° × 12.5° resolution) for the entire globe and El-Niño 3.4 region (5°S–5°N; 120°W–170°W) we have 105 grid points with (2.5° × 2.5° resolution). If a single label is used to label the points on the grid (details below), the El Niño basin (ENB) region corresponds to the 365th to the 368th label of the 725 grid points of the global grid. The ENB region is inside the equatorial Pacific region (20°N–20°S, 100°E–60°W, with node labels 299 to 431 in our labelling scheme).

We obtained monthly correlations during the arrival of the El Niño or La Niña events and for the preceding month to the event, both for the entire globe and for the ENB region and constructed the heat map. This is done by calculating the correlation coefficient, as defined in eq. (2) between the nodes of the grid, with $\tau = 0$, using the measured temperature $\tilde{T}_i$ and calculating the average over the days of the given month. To label the indices of a row of the correlation matrix, we use the nested loop of longitudes within all the latitudes, i.e. the row index is ordered by all longitudes, for a given latitude, and then by the next latitude. Thus each geographic grid point is now represented by a single index in each row, say i, where $i = 1, \ldots, 725$ for the global grid. The columns are ordered in the same way. The correlation values between pairs of geographic points, where the geographic points now have these single labels, are used as the elements of the adjacency matrix which is then visualised as a heat map [12].

Here, our heat map is a two-dimensional display of the adjacency matrix in which the correlation values associated with individual elements or cells are displayed via a color palette. Thus, the color gradient of a cell as well as the entire heat map are determined by the correlation amplitude between pairs of nodes. We can also use the correlation matrix to calculate quantifiers like the fraction of links with correlation values above a certain threshold, and the transitivity. The definition of transitivity is based on triplets of nodes. A triplet is three nodes connected by either two (open triplet) or three (closed triplet) undirected ties. Therefore, a triangle graph includes three closed triplets, one centered on each of the nodes (i.e. the three triplets in a triangle come from overlapping selections of nodes). Transitivity is the number of closed triplets (or 3 × triangles) over the total number of triplets (both open and closed). This measure indicates the clustering in the whole network (global) [13]. Thus, transitivity = (no. of closed triplets)/[no. of all triplets (open or closed)].

We exhibit the heat maps of an El Niño event, and a La Niña event here, both for the global grid, and for the El Niño region. The heat maps are organized along the diagonal. The block structure of the correlation displays distinct behavior for the El Niño and La Niña episodes. A very strong El Niño event of duration April '82 to July '83 was seen in 1982 [11]. On the arrival of the El-Niño event, we calculated the percentage of higher correlation values (0.5–1.0) for the entire globe for the months of February, March and April. The values are 11.699, 11.833 and 28.498 percent, respectively. For the ENB region the percentages of higher correlation values

Table 1. Year 1982 (very strong El Niño).

Three months overlap	ONI	Month	Percentage of strong links	Transitivity
December–January–February	0.0			
January–February–March	0.1	February	11.699	0.620
February–March–April	0.2	March	11.833	0.661
March–April–May	0.5	April	28.498	0.735
April–May–June	0.7			

Table 2. Year 1991 (strong El Niño).

Three months overlap	ONI	Month	Percentage of strong links	Transitivity
January–February–March	0.3			
February–March–April	0.2	Mar	17.589	0.662
March–April–May	0.3	April	26.125	0.800
April–May–June	0.5	May	29.867	0.753
May–June–July	0.6			

(0.75–1.0) are 32.580, 37.623 and 59.446 respectively. These values, as well as the values for the transitivity for the global grid and the ONI are listed in table 1. We also show the same quantities in table 2 for the year 1991, which was a strong El Niño year.

The heat map for the year 1982 can be seen in figure 4 for both the global grid and the ENB.

The year 2008 had a weak La Niña event of duration: November '08 to March '09. The 2008 La Niña is a weak event because the maximum ONI is −0.8. On the arrival of the La Niña (2008) event we calculated the percentage of higher correlation values (0.5–1.0) for the entire globe for the months of September, October and November. The values are 39.485 and 22.510 and 16.771, respectively. These values and the corresponding transitivity values are listed in table 3 along with the ONI. Table 4 lists the same quantities for the year 2007, a strong La Niña year.

We plot the heat map for the year 2008 in figure 5, again for the global grid and the ENB. For the ENB region the percentage of higher correlation values (0.75 to 1.0) is 46.984, 25.342 and 37.932, respectively. The

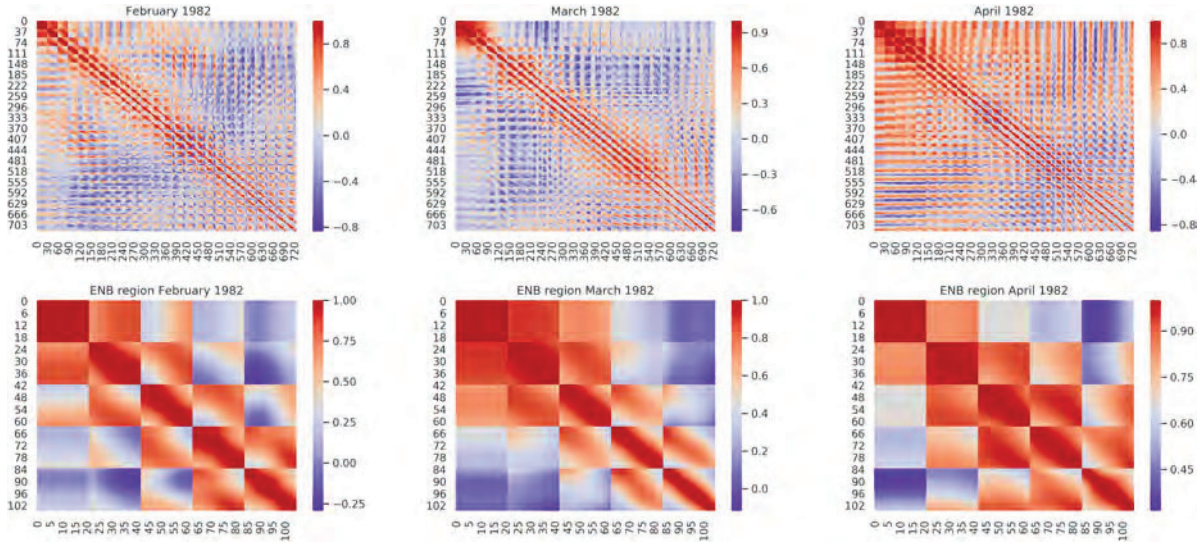

Figure 4. Very strong El Niño year 1982. On the arrival of the El Niño event, the percentage of higher correlation values (0.5 to 1.0) for the entire globe for the months of February, March and April are 11.699, 11.833 and 28.498, respectively. Similarly for the ENB region, the percentage of higher correlation values (0.75–1.0) are 32.580, 37.623 and 59.446, respectively. The ENB region corresponds to the labels 365 to 368 on both axes on the global heat map but is plotted with a finer resolution (see text).

Table 3. Year 2008 (weak La Niña).

Three months overlap	ONI	Month	Percentage of strong links	Transitivity
July–August–September	–0.3			
August–September–October	–0.3	September	39.845	0.737
September–October–November	–0.4	October	22.510	0.623
October–November–December	–0.6	November	16.771	0.605
November–December–January	–0.7			

Table 4. Year 2007 (strong La Niña).

Three months overlap	ONI	Month	Percentage of strong links	Transitivity
Mar–Apr–May	–0.2			
April–May–June	–0.3	May	50.353	0.837
May–June–Jul	–0.4	June	30.354	0.775
June–July–August	–0.5	July	10.432	0.646
July–August–September	–0.8			

values of the transitivity are 0.805, 0.779 and 0.768, respectively.

We compare the behavior of the quantities of interest, viz. The percentage of strong links and the transitivity for the global grids for the La Niña and El Niño years for the global grid, with years where no event is seen. Tables 5 and 6 show the behavior of these quantities for two years, 1990 and 1993, where no such event is seen.

The heat map of the neutral years also shows different behavior from that seen for the El Niño and La Niña years. We plot the heat map of the year 1993 where no event occurs in figure 6 [14].

During the onset of the very strong El Niño for the month of April 1982 we get the highest percentage of strong links displayed via the color palette in the heat map. For the weak La Niña we find the highest percentage of strong links during the months of September and October. Thus during the onset of the El Niño and La Niña we get a high percentage of strong links in one or more of the previous months. However, for the period where no event is seen, and the ONI is almost unchanged (November 1993 to January 1994), we do not get any signal in the heat map (almost uniform values of high correlation throughout the period). We note that the transitivity shows no consistent trend for any of the cases studied, either for the global grid or for the ENB. We have also noted this behavior in the cluster coefficients for the networks, for both the

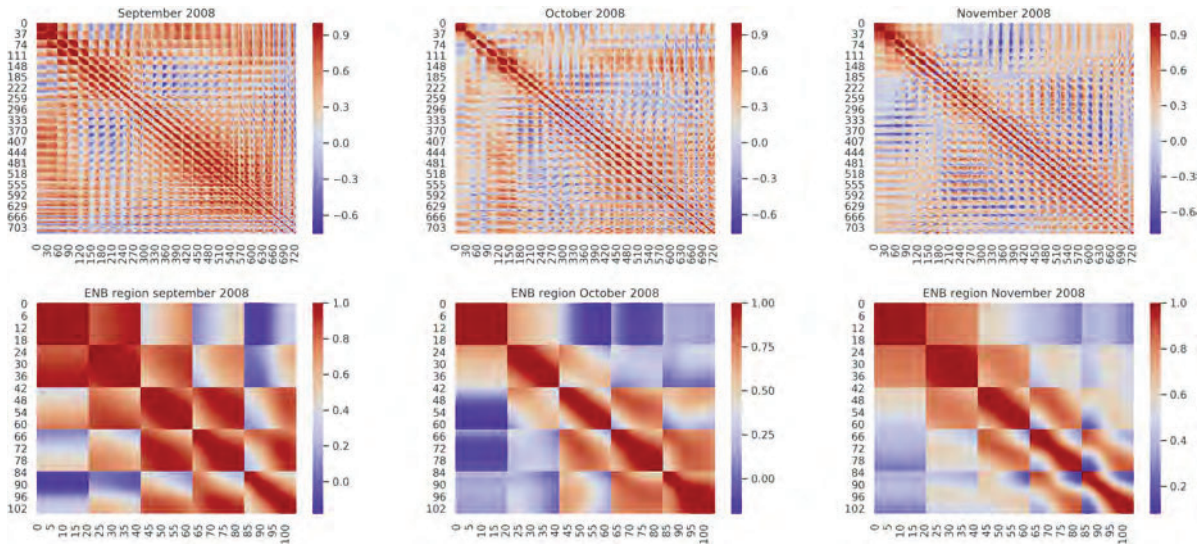

Figure 5. Weak La Niña year 2008. On the arrival of the La Niña event the percentage of higher correlation values (0.5–1.0) for the entire globe for the months of September, October and November are 39.845 and 22.510 and 16.771, respectively. For the ENB region the percentage of higher correlation values (0.75–1.0) are 46.984, 25.342 and 37.932, respectively.

Table 5. Year 1990 (no event: fixed ONI (0.3) for sufficient time duration).

Three months overlap	ONI	Month	Percentage of strong links	Transitivity
April–May–Jun	0.3			
May–June–July	0.3	June	20.438	0.622
June–July–August	0.3	July	14.135	0.592
July–August–September	0.4	August	20.278	0.645
August–September–October	0.4			

Table 6. Year 1993–1994 (no event: fixed ONI 0.1 for sufficient time duration).

Three months overlap	ONI	Month	Percentage of strong links	Transitivity
September–October–November	0.1			
October–November–December	0.0	November	20.548	0.686
November–December–January	0.1	December	10.587	0.593
December–January–February	0.1	January 94	9.209	0.725
November–December–January	0.1			

global and ENB cases, although this quantity is not listed here.

The heat maps of the three events show gradual evolution in the strength of the links. In all cases the structure is organised along one of the diagonals. For the 1982 very strong event, the block with the strongest correlations can be seen on the top left of the figure in February. In March, the strong links spread and two distinct blocks and a set of overlapping blocks are seen in the figure. In April, the strong links spread, and the left upper triangle shows a large number of strongly correlated links. The heat maps for the ENB show similar behavior. In the case of La Niña of 2008, the pattern in the months of onset (September, October and November) is quite different. Overlapping blocks of strong correlation are seen in September, they shrink in size and spread in October and reduce further in November. This is in contrast with the El Niño which shows an increasing trend. The heat maps of the ENB region show similar behavior. The neutral year (1993) shows three prominent blocks in the month of November. These reduce in size, in December, and diffuse by January 1994. The same behavior is seen in the quantifiers, as well as in the ENB basin. We call this a neutral year as no consistent anomaly is seen for three overlapping periods. We expect that the small anomaly mentioned in Ref. [15] (May 1993)

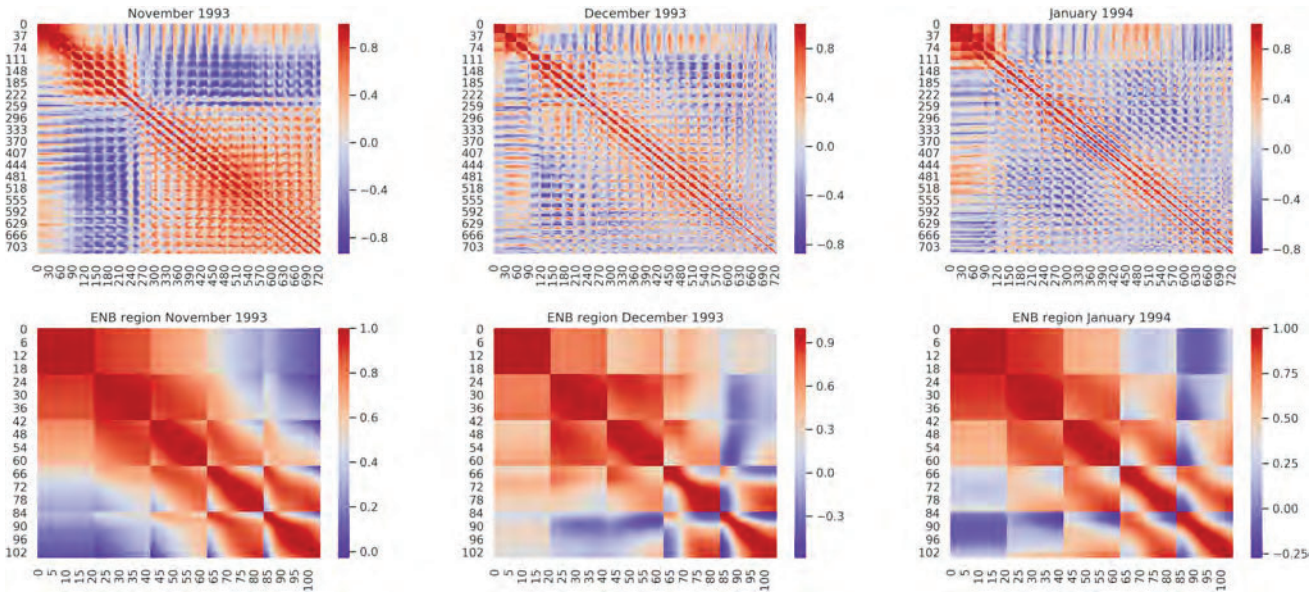

Figure 6. The year 1993 is a neutral year. We choose the months November, December of 1993 and January 1994 based on the ONI. For these three months and the following two months the ONI value is constant (0.1). We calculated the percentage of higher correlation values (0.5–1.0) for the entire globe for the months of November, December '93 and January '94. The values are 20.548, 10.587 and 9.209, respectively. For the ENB region, the percentage of higher correlation values (0.75–1.0) are 44.317, 23.383 and 43.069, respectively.

will be picked up by our methods. We will verify this elsewhere.

We have observed similar behavior in other years as well. Thus the correlation matrix of the network shows a structure which has distinct characteristics of El Niño events, La Niña events, and no events. It is clear that the heat maps are highly sensitive to changes in ONI, as can be seen from the block structure, as well as from the percentage of highly correlated links which increase consistently during the onset of the El Niño and decrease consistently in the onset of the La Niña. Further characterisation of the heat maps using quantities like the modularity and the identification of nodes of high degree may uncover teleconnections and tipping points. We hope to carry this out in future work.

To summarise, percolation networks obtained from climate data show signatures of major climatic phenomena. We have demonstrated this for cyclonic data and El Ninõ and La Ninã data. Further quantification of these networks using topological events and patterns of microtransitions [9] is in progress. We hope these properties can be further used for the prediction of these events.

Acknowledgements

The authors thank Shraddha Gupta for discussion and preliminary work [16] on the cyclone aspects of this paper. NG thanks DST-DAAD for a DST-DAAD project and RS thanks IIT Madras for an Institute Postdoctoral Fellowship.

References

[1] J Meng, J Fan, Y Ashkenazy and S Havlin, *Chaos* **27**, 035807 (2017)

[2] K Yamasaki, A Gozolchiani and S Havlin, *Phys. Rev. Lett.* **100**, 228501 (2008)

[3] A A Tsonis, K L Swanson and P J Roebber, *Bull. Am. Meteorol. Soc.* **87**, 585 (2006)

[4] N Malik, B Bookhagen, N Marwan and J Kurths, *Clim. Dyn.* **39**, 971 (2012)

[5] V Stolbova, E Surovyatkina, B Bookhagen and J Kurths, *Geophys. Res. Lett.* **43**, 3982 (2016)

[6] The European Centre for Medium-Range Weather Forecasts (ECMWF) is an independent intergovernmental organisation, http://apps.ecmwf.int/datasets/data/interim-full-daily/levtype=pl/

[7] R Albert and A L Barabási, *Rev. Mod. Phys.* **74**, 1 (2002)

[8] R Sonone and N Gupte, arXiv preprint, arXiv:2002.04530 (2020)

[9] N Gupte, A Roy and R Sonone, *Indian Acad. Sci. Conf. Ser.* **2**, 151 (2019)

[10] V Rodríguez-Méndez, V Eguíluz, E Hernández-García and J Ramasco, *Sci. Rep.* **6**, 29552 (2016)

[11] The ONI threshold is further broken down into weak (with a 0.5–0.9 SST anomaly), moderate (1.0–1.4), strong (1.5–1.9) and very strong (2.0) events, https://ggweather.com/enso/oni.htm

[12] L Wilkinson and M Friendly, *Am. Stat.* **63**, 2 (2009)

[13] R D Luce and A D Perry, *Psychometrika* **2**, 14 (1949)

[14] El Niño and La Niña events are defined as at least 5 consecutive overlapping 3-month periods at or above the +0.5 anomaly for warm (El Niño) events and at or below the −0.5 anomaly for cold (La Niña) events (https://ggweather.com/enso/oni.htm). For 1993 the ONI increased to 0.7 in the month of May, but it did not last for at least 5 months, so by definition it is a neutral year

[15] W S Kessler, *Geophys. Res. Lett.* **29**, 40 (2002)

[16] S Gupta, *M.Sc. project* (Department of Physics, IIT Madras, 2018)